

2x Current Boosting Scheme in 3300 V 4H-SiC VDMOSFET

Yuniarto Widjaja^{1,a*}, Valerii Nebesnyi^{1,b}, Oleksandr Maistriuk^{1,c},
Asen Asenov^{1,2,d}, Nikolas Xeni^{2,e}, Tapas Dutta^{2,f}, Djamel Bensouiah^{2,g},
Servin Rathi^{3,h}, Leo Laborie^{3,i}, Robert Young^{3,j}, Yunyi Qi^{3,k}
and David T. Clark^{3,l}

¹Volta Semiconductor, Inc., Cupertino, CA, USA

²Semiwise Ltd., Glasgow, UK

³Clas-SiC Wafer Fab Ltd., Lochgelly, UK

^{a*}ywidjaja@voltasemi.com, ^bvn@voltasemi.com, ^com@voltasemi.com,

^dasen.asenov@semiwise.uk, ^enikolas.xeni@semiwise.uk, ^ftapas.dutta@semiwise.uk,

^gdjamel.bensouiah@semiwise.uk, ^hservin.rathi@clas-sic.com, ⁱleo.laborie@clas-sic.com,

^jrobert.young@clas-sic.com, ^kkelly.qi@clas-sic.com,

^ldavid.clark@clas-sic.com

Keywords: 3300 V, silicon carbide, low specific on-resistance, on-current improvement, p-well bias.

Abstract. We experimentally demonstrated a $\sim 2x$ on-current enhancement in VDMOSFET fabricated in a standard 3300 V-rated 4H-SiC process. The on-current improvement is achieved by applying a positive bias to the p-well region when the VDMOSFET is in the on-state. A $5 \times 10^3 - 10^4$ ratio between the on-current gain and the p-well current gain is shown. TCAD simulations are performed to study the underlying mechanisms of the on-current gain.

Introduction

Wide bandgap (WBG) semiconductors, such as silicon carbide (SiC), have been increasingly utilized in high-voltage, high-power applications due to advantages in electrical and thermal properties over silicon. Low conduction losses is one of the requirements of power semiconductor applications and therefore there are many efforts to improve the on-current and specific on-resistance of SiC devices, for example through process improvements [1-3], cell topologies [4], and charge modulations [5]. Previously, we demonstrated a $>2.5x$ on-current improvement in 1200 V-rated 4H-SiC based MOSFET through the application of p-well voltage [6]. 3300 V-rated devices have received significant interest for solid-state transformers, industrial and traction applications. In this work, we demonstrated a $\sim 2x$ on-current enhancement resulting from p-well voltage biasing in 3300 V-rated 4H-SiC based VDMOSFET.

Figure 1(a) illustrates a schematic cross-sectional view of our VDMOSFET device, which is fabricated in a standard 3.3 kV 4H-SiC process on 150 mm wafers. The details of the fabrication process are described in [7] and a breakdown voltage of 3950 V is achieved (Figure 1(b)).

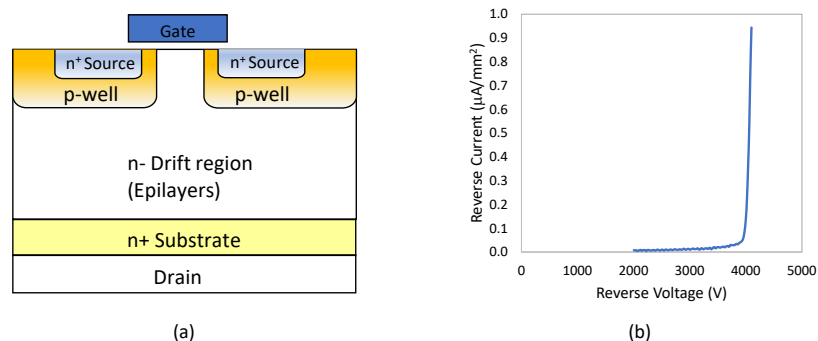


Fig. 1. (a) Cross-sectional view of device structure, **(b)** Breakdown characteristic of a typical 3300V device.

Separate contacts are formed for the p-well and source regions, allowing for independent biasing of both regions (p-well contact is not shown in Figure 1(a)). A positive bias is applied to the p-well region when the VDMOSFET is in the on-state and removed when it is in the off-state. In a conventional VDMOSFET, the p-well and source regions are shorted and typically connected to a common ground.

Results and Discussion

Figure 2(a) shows the I_d - V_g curves measured from a test structure having a JFET width of $15\ \mu\text{m}$ for different V_p and drain voltage (V_d). The ratio of the drain current with $V_p=2.2\text{V}$ and $V_p=0\text{V}$ for a range of gate voltage (V_g) is shown in Figure 2(b), demonstrating $\sim 2\times$ on-current when $V_p=2.2\text{V}$ is applied compared to conventional VDMOSFET (with $V_p=0\text{V}$). The ratio of the on-current as a function of applied V_p bias is also shown in Figure 2(c), indicating that the current flow across the VDMOSFET can be controlled by both V_g and V_p . When the VDMOSFET is turned off, the positive V_p bias is removed and the off-state characteristics return to those with $V_p=0\text{V}$ applied. In addition, the application of V_p bias has been shown to reduce both the variability of the threshold voltage and the time-dependent threshold voltage drift [8, 9].

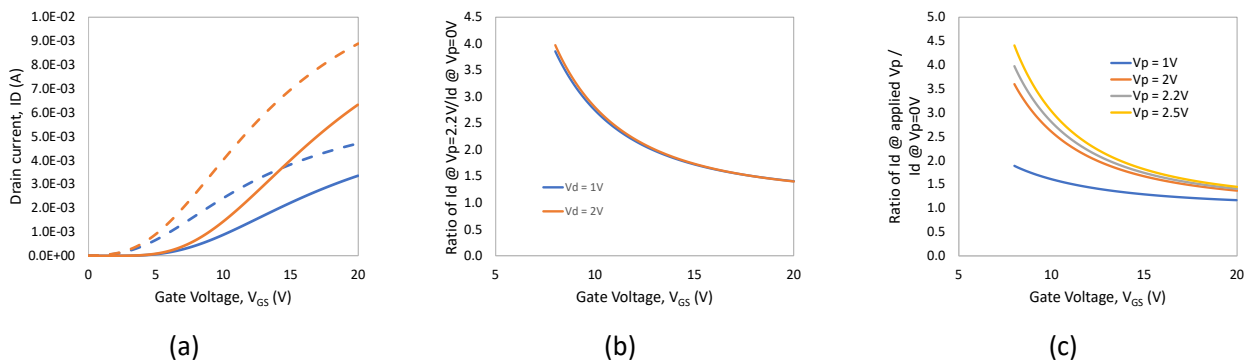


Fig. 2. (a) I_d - V_g characteristics of VDMOSFET for $V_d=1\text{V}$ and 2V with $V_p=0\text{V}$ (solid) and $V_p=2.2\text{V}$ (dashed), (b) Ratio of drain current with $V_p=2.2\text{V}$ and $V_p=0\text{V}$ applied, (c) Ratio of drain current at different applied V_p and $V_p=0\text{V}$ for $V_d=2\text{V}$.

Kimoto and Watanabe have previously shown that the drift resistance accounts for $\sim 80\%$ of the on-resistance of $3300\ \text{V}$ SiC power MOSFET [10]. The p-well current is measured to study whether the significant on-current gain can be attributed to the vertical BJT device. Figure 3(a) provides the ratio of the on-current gain to the p-well current (i.e. the BJT gain). A high ratio of 5×10^3 - 10^4 is observed, demonstrating that the large current gain does not require a large p-well current. The improvement in the channel resistance is investigated by measuring the transconductance (g_m). Figure 3(b) shows a $\sim 30\%$ higher peak g_m with $V_p=2.2\text{V}$. The I_d - V_g and g_m show that threshold voltage (V_t) shift and g_m contribute to the on-current gain.

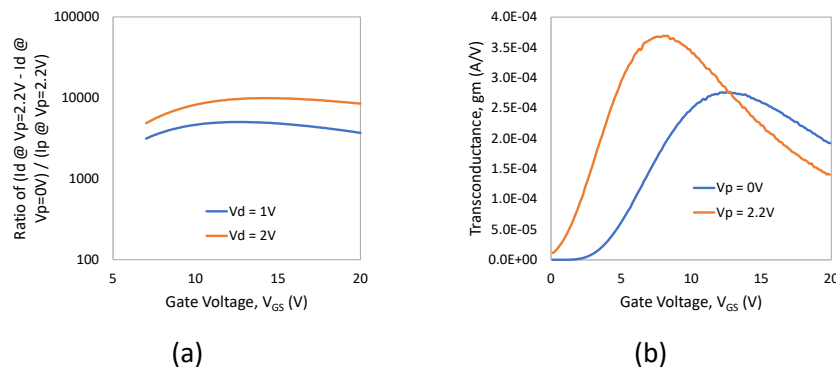


Fig. 3. (a) Ratio of current gain (the difference between drain current with $V_p=2.2\text{V}$ and 0V) and p-well current for $V_d=1\text{V}$ and 2V , (b) Transconductance (g_m) for $V_d=2\text{V}$ with $V_p=2.2\text{V}$ and 0V .

TCAD simulations are performed to further study the underlying mechanisms of the drain on-current gain. The TCAD simulations have been calibrated using the experimental results from the 1.2 kV 4H-SiC process and adjusted to account for the differences between the 3.3 kV and 1.2 kV processes. Figure 4 illustrates a comparison of the I_d - V_g characteristics of the 3.3 kV device under $V_p=0V$ and $V_p=2.2V$ bias conditions. As shown in Figure 4, TCAD simulations also show a $\sim 2x$ on-current, consistent with the experimental results.

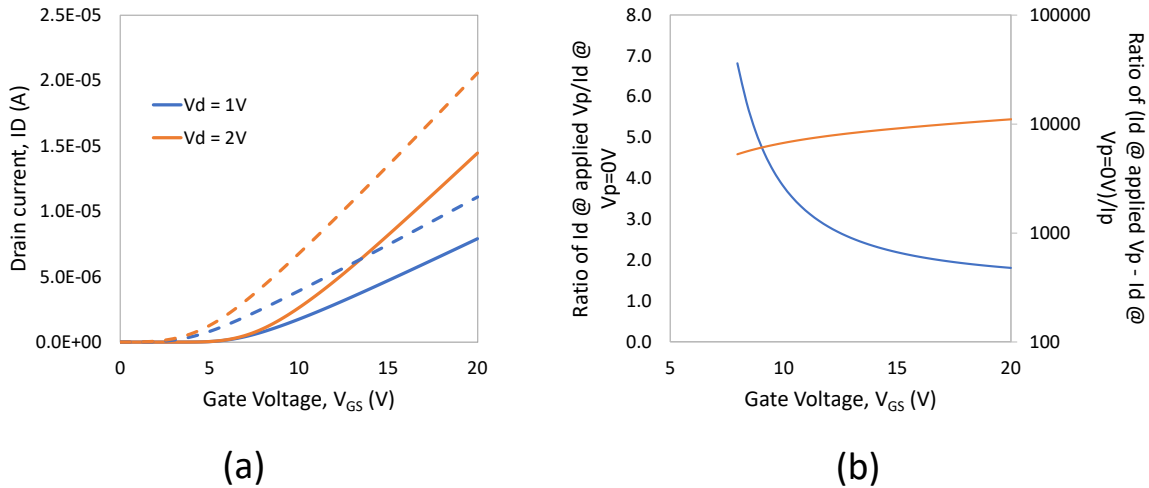


Fig. 4. (a). TCAD simulation I_d - V_g characteristics of VDMOSFET for $V_d=1V$ and $2V$ with $V_p=0V$ (solid) and $V_p=2.2V$ (dashed), (b) TCAD optimization results showing drain current gain (left axis) and the ratio of current gain to p-well current (right axis).

Figure 5(a) illustrates a cross section of the energy band diagram along the source/p-well/drift region junctions with $V_p=0V$ and $V_p=2.2V$ bias applied. Applying a positive V_p bias lowers the energy barrier between the source and the p-well regions, increasing current flow through the p-well region. A comparison of the current density plots shows that a higher current density is observed throughout the source junction region and is not limited to only the area near the surface channel when a positive bias is applied to the p-well. Electron flow in the region away from the surface area is not limited by the poor channel mobility of SiC, and as a result, a higher effective mobility, μ_{eff} is obtained, as observed by the higher transconductance shown in Figure 3(b). This is similar to the effect of on-resistance improvement through the formation of current spreading layer (CSL) or deep JFET layer shown by Jang et al. [11] and Kim et al. [12], respectively.

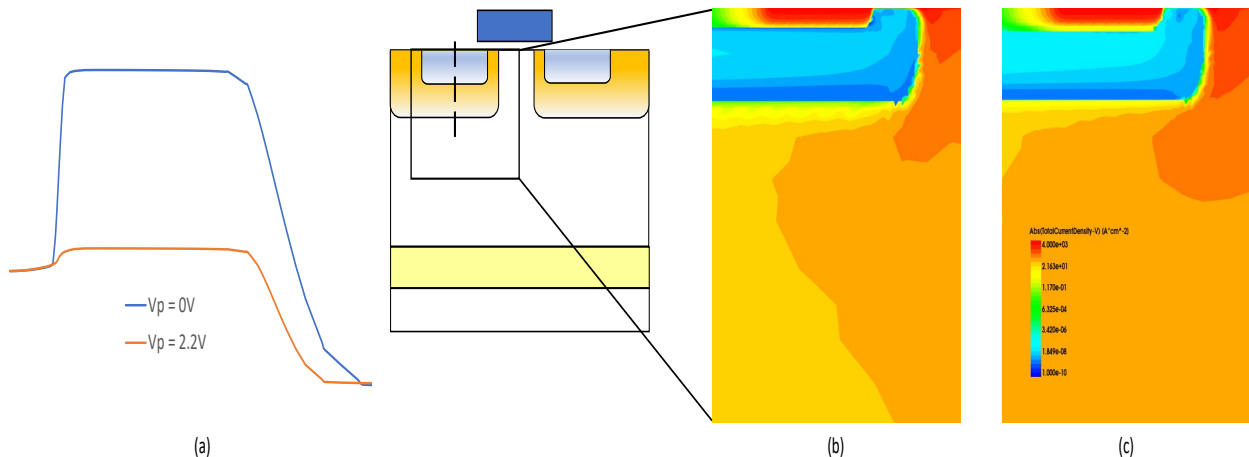


Fig. 5. TCAD simulation results showing (a) the energy band diagram across the region indicated by the dashed line, and total current density in the VDMOSFET region enclosed by the box for (b) $V_p=0V$ and (c) $V_p=2.2V$.

TCAD simulations are also used to further optimize the 3.3 kV device. As shown in Figure 4(b), a higher on-current can be achieved through further device structure optimizations, while maintaining 5×10^3 - 10^4 ratio between on-current gain and the p-well current. This is accomplished by further increasing the conduction area to encompass a larger portion of the source area.

The specific on-resistance is shown in Figure 6 alongside selected 3.3 kV results [13-15] and our previous 1.2 kV results [6], demonstrating that the p-well biasing results approach the SiC limit [16].

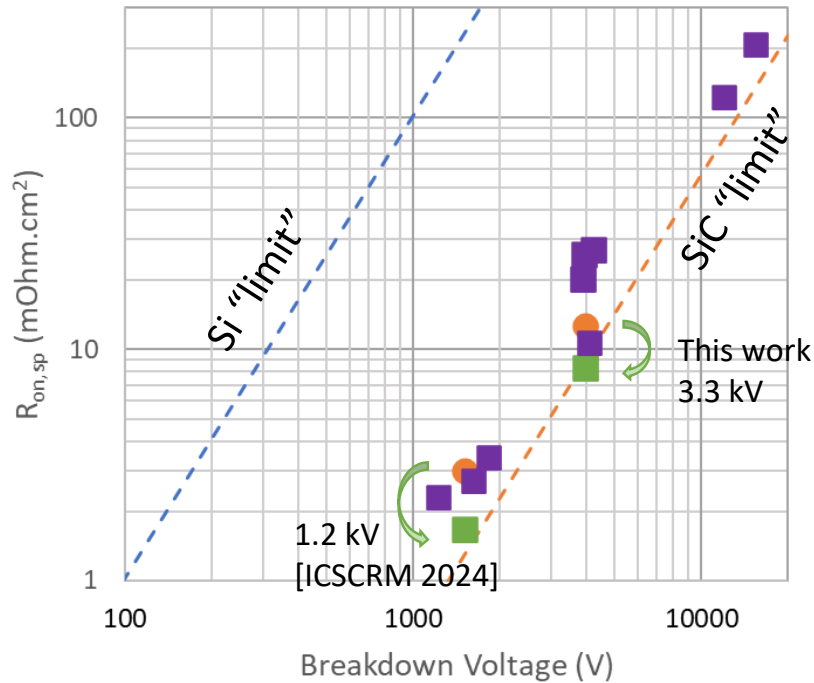


Fig. 6. Specific on-resistance vs. breakdown voltage, showing p-well boosting approaches the SiC limit.

Summary

A $\sim 2x$ improvement in the on-current of 3300 V-rated 4H-SiC VDMOSFETs has been demonstrated. The current gain is achieved through the application of a positive bias to the p-well region. The application of the p-well bias does not result in significant increase in the p-well current, where a ratio of 5×10^3 - 10^4 between the on-current gain and the p-well current is observed. The specific on-resistance demonstrates that the p-well biasing yield results approaching the SiC limit. TCAD simulations are performed to understand the current boosting mechanism and to investigate further optimizations.

Acknowledgement

The authors would like to thank Ian Widjaja for contributions to TCAD simulations, as well as Christopher Norwood, Kuk-Hwan Kim, and Valentin Abramzon for insightful discussions.

Author Contribution

YW: conceptualization (equal), writing – original draft (lead), formal analysis (lead), writing – review and editing (equal).

VN: conceptualization (equal), formal analysis, writing – review and editing (equal).

OM: formal analysis, writing – review and editing (equal).

AA: conceptualization (equal), formal analysis, writing – review and editing (equal).

NX: data curation (equal), investigation – simulation (equal), writing – review and editing (equal).

TD: data curation (equal), investigation – simulation (equal), writing – review and editing (equal).
DB: data curation (equal), investigation – simulation (equal), writing – review and editing (equal).
SR: data curation (equal), investigation – device layout, process, test (equal), writing – review and editing (equal).
LL: data curation (equal), investigation – device layout, process, test (equal), writing – review and editing (equal).
RY: data curation (equal), investigation – device layout, process, test (equal), writing – review and editing (equal).
YQ: data curation (equal), investigation – device layout, process, test (equal), writing – review and editing (equal).
DTC: data curation (equal), formal analysis, investigation – device layout, process, test (equal), writing – review and editing (equal).

References

- [1] Uchida, Kosuke, et al. “The optimised design and characterization of 1200 V/2.0 mΩ cm² 4H-SiC V-groove trench MOSFETs.” 2015 IEEE 27th International Symposium on Power Semiconductor Devices & IC's (ISPSD). IEEE, 2015.
- [2] Kim, Dongyoung, et al. “The effect of deep JFET and P-well implant of 1.2 kV 4H-SiC MOSFETs.” IEEE Journal of the Electron Devices Society 10 (2022): 989-995.
- [3] Kim, Jeff Joohyung, et al. “Investigation into Relationship of the Switching Performance and Short-Circuit Withstand Time on 1.2 kV 4H-SiC Power MOSFETs.” 2024 36th International Symposium on Power Semiconductor Devices and ICs (ISPSD). IEEE, 2024.
- [4] Han, Kijeong, and B. J. Baliga. “Comparison of four cell topologies for 1.2-kV accumulation- and inversion-channel 4H-SiC MOSFETs: Analysis and experimental results.” IEEE Transactions on Electron Devices 66.5 (2019): 2321-2326.
- [5] Masuda, Takeyoshi, et al. “Challenges in Extremely Low Specific On-Resistance with SiC SJ-VDMOSFETs.” Materials Science Forum. Vol. 1004. Trans Tech Publications Ltd, 2020.
- [6] Widjaja, Yuniarto, et al. “1200 V 4H-SiC VDMOSFET Having > 2.5x On-Current Improvement.” International Conference on Silicon Carbide and Related Materials (2024): 530-531.
- [7] S. Rathi, D. Macdonald, A. Murphy, M. Bell, R. Young, and D. Clark, “Influence of Channel Length and Gate Oxide Thickness Variations in 3300 V 4H-SiC VDMOSFET.” International Conference on Silicon Carbide and Related Materials (2023).
- [8] Franco, Jacopo, et al. “Reduction of the BTI time-dependent variability in nanoscaled MOSFETs by body bias.” 2013 IEEE International Reliability Physics Symposium (IRPS). IEEE, 2013.
- [9] Walth, Michael, et al. “Evaluation of the impact of body bias on the threshold voltage drift of planar SiO₂ transistors.” Microelectronics Reliability 168 (2025): 115693.
- [10] Kimoto, Tsunenobu, and Heiji Watanabe. “Defect engineering in SiC technology for high-voltage power devices.” Applied Physics Express 13.12 (2020): 120101.
- [11] Jang, Seung Yup, et al. “Improved on-state resistance with reliable reverse characteristics in 1.2 kV 4H-SiC MOSFET by selective nitrogen implantation assisted current spreading layer.” Japanese Journal of Applied Physics 59.4 (2020): 046501.
- [12] Kim, Dongyoung, et al. “The effect of deep JFET and P-well implant of 1.2 kV 4H-SiC MOSFETs.” IEEE Journal of the Electron Devices Society 10 (2022): 989-995.

- [13] Palmour, John W., et al. "Silicon carbide power MOSFETs: Breakthrough performance from 900 V up to 15 kV." 2014 IEEE 26th International Symposium on Power Semiconductor Devices & IC's (ISPSD). IEEE, 2014.
- [14] Zhang, Luyang, et al. "Comparison of a 3.3 kV SiC Hybrid-Channel Trench MOSFET and a Planar MOSFET." 2022 IEEE Workshop on Wide Bandgap Power Devices and Applications in Europe (WiPDA Europe). IEEE, 2022.
- [15] Chen, Ximing, et al. "Different JFET designs on conduction and short-circuit capability for 3.3 kV planar-gate silicon carbide MOSFETs." IEEE Journal of the Electron Devices Society 8 (2020): 841-845.
- [16] Baliga, B. Jayant. "Fundamentals of Power Semiconductor Devices." Springer, Berlin (2008).